ISSN 0027-1349

*Moscow University*

# Physics Bulletin

*(Vestnik Moskovskogo Universiteta. Fizika)*

Vol. 50, No. 6

ALLERTON PRESS, INC.

*Moscow University Physics Bulletin*
*Vol. 50, No. 6, pp. 35–40, 1995*

*Vestnik Moskovskogo Universiteta. Fizika*
*UDC 534.222*

# SHOCK WAVE EFFECT ON RESONANCE SOUND ABSORBERS

A. A. Zaikin and O. V. Rudenko

**The nonlinear distortion of the spectrum of a sound shock wave propagating through the atmosphere is analyzed. The pressure waveforms of the reflected and transmitted pulses are calculated as a shock perturbation hits an acoustic resonance system which models elements of sound-absorbing and sound-proofing structures.**

The problem of reducing the levels of intensive noises and shock waves, harmful to living organisms, has become especially important in recent years due to growing traffic intensity and development of supersonic transport. The inadmissively high level of the sound shock wave created by supersonic aircraft when flying over densely populated areas is almost the only reason capable of interfering with the implementation of projects for building new-generation supersonic passenger aircraft [1, 2].

Various possibilities of reducing the adverse effect of this wave are currently under study. They include both changing the vehicle configurations, appropriate route selection and maneuver restriction, and the use of sound-absorbing screens, helmets and other means of individual protection.

Acoustic resonance systems can be used as sound-absorbing and sound-proofing structural elements. One of the advantages of resonance sound absorbers is their low-frequency absorption characteristic [3]. Therefore, the use of acoustic resonators in the low-frequency and infrasound bands was proposed in [4]. The problem of shock wave incidence upon a Helmholtz resonator was solved numerically in [5], but the $N$-shaped wave, which models a sound shock, was not considered.

In [6], asymptotic methods of nonlinear acoustics were used to calculate the profile of a sound-shock wave (i.e., its pressure waveform), and the structure of the shock fronts was described in detail. It is well known that the effect of a strong acoustic pulse depends on many of its characteristics, including the maximum peak pressure, the pressure gradient at the front, and the corresponding parameters of the rarefaction wave. Furthermore, since biological objects possess some characteristic "dangerous" frequencies, the sound shock wave spectrum must be calculated in both low- and high-frequency regions.

The wave propagation can be described by the equation

$$\frac{\partial V}{\partial z} = V\frac{\partial V}{\partial \theta} + \Gamma\frac{\partial^2 V}{\partial \theta^2}. \tag{1}$$

Here $V = p/p_0$ is the acoustic pressure divided by the pulse peak pressure, $\theta = (t - s/c_0)/t_0$ is the time in the coordinate system which moves with the pulse at the velocity of sound $c_0$, $t_0$ is the pulse duration, $z = \varepsilon p_0 s/(\rho_0 c_0{}^3 t_0)$ is the distance divided by the length of discontinuity formation. In the last formula, $s$ is the distance counted generally along a curvilinear ray in a nonuniform atmosphere, $\varepsilon$ is the nonlinearity parameter, $\rho_0$ is the characteristic value of the medium density. The number $\Gamma = bt_0/(2\varepsilon p_0)$ is the reciprocal acoustic Reynolds number, equal to the ratio of the absorption and discontinuity formation lengths. The effective dissipative parameter $b = \xi + (4/3)\eta + (c_v^{-1} - c_p^{-1})\chi$ is expressed in terms of the coefficients of the shear $\eta$ and the volume $\xi$ viscosities and the heat conductivity $\chi$.

For an initial perturbation in the form of an $N$ pulse with an infinitely narrow front, the following

solution was derived in [6]

$$\frac{p}{p_0} = \frac{1}{2\sqrt{1+2z}}\left(\tanh\frac{\theta+\theta_1}{8\Gamma\theta_1}+1\right), \quad \theta < -\theta_1(z) = -\frac{1}{2}\sqrt{1+2z},$$
$$\frac{p}{p_0} = -\frac{2}{1+2z} + \frac{1}{4\theta_1}\left(\tanh\frac{\theta+\theta_1}{8\Gamma\theta_1}-1\right)$$
$$+\frac{1}{4\theta_1}\left(\tanh\frac{\theta-\theta_1}{8\Gamma\theta_1}+1\right), \quad -\theta_1 < \theta < \theta_1, \tag{2}$$
$$\frac{p}{p_0} = \frac{1}{4\theta_1}\left(\tanh\frac{\theta-\theta_1}{8\Gamma\theta_1}-1\right), \quad \theta > \theta_1.$$

The solution is an $N$ pulse with a front of finite width and a duration which depend on the distance. The width depends on the reciprocal Reynolds number: the larger $\Gamma$, the wider the shock front. In particular, the front widening is due to the effect of molecular relaxation of the gas components ($O_2$ and $N_2$) in the upper layers of the atmosphere, as well as to the presence of water vapor and drops (i.e., clouds). An interesting fact is that in the vicinity of the initial discontinuity (near $\theta = \pm\theta_1(z)$) the solution behaves like an exponential with a linear exponent in $\theta$, rather than a quadratic exponent as was believed earlier.

Let us now discuss those characteristics of the $N$ wave which are important for evaluating its effect upon various objects. The foremost of them are $p_0(z)$ and $t_0(z)$, the peak perturbation of pressure and the pulse duration, which in actual conditions amount to about 100 Pa and 0.1 s, respectively. Propagating in the atmosphere, the wave is transformed as follows: the peak pressure falls with increasing distance and the $N$ pulse duration grows; this is easily seen from asymptotic solution (2).

A very important parameter is the pressure gradient, or the shock front steepness, evaluated as

$$\left(\frac{\partial p}{\partial z}\right)_{\max} = \frac{p_0}{2\Gamma c_0 t_0}. \tag{3}$$

When studying the effects on biological objects, the information on the frequency spectrum is also important. For instance, very harmful for humans are the infrasound band and resonance frequencies (e.g., those which are close to the characteristic frequencies of intracraneal structures). The spectrum which conforms with the solution (2) has the form

$$\left|\frac{p(n=\omega t_0)}{p_0}\right| = \frac{1}{\theta_0}\left|4\pi\Gamma\theta_1\frac{\cos(n\theta_1)}{\sinh(4\pi\Gamma n\theta_1)} - \frac{1}{n^2\theta_1}\sin(n\theta_1)\right|. \tag{4}$$

A typical shape of spectrum (4) is depicted in Fig. 1 (curve 1, $\Gamma = 0$). Its maxima are located in the low-frequency region. However, a significant portion of the energy also falls into the high-frequency area, which corresponds to the steep fronts in the signal profile.

The picture becomes different for a finite dissipation ($\Gamma \neq 0$) and thus a finite duration of the shock front. The spectrum now has an upper boundary frequency; the entire spectrum is displaced toward lower frequencies, and the heights of its maxima are changed. The way the spectrum changes at different values of $\Gamma$ is also shown in Fig. 1, where curve 2 corresponds to $\Gamma = 0.05$, curve 3 to $\Gamma = 0.1$, and curve 4 to $\Gamma = 0.2$.

Calculations by formula (4) show that the spectrum of a pulse which propagates in the atmosphere "shrinks" with distance, shifting toward lower frequencies. The spectral maxima become closer to each other, but their magnitudes remain unchanged.

We now turn to numerical estimates. For air at a temperature of 0°C and a pressure of 1 atm, we assume the shear viscosity to be $\eta = 1.72 \times 10^{-5}$ Pa s, the heat conductivity $\chi = 0.23$ J K/kg, the heat capacities $c_p = 1004.8$ and $c_v = 716.15$ J K/kg, $b = 11.5 \times 10^{-5}$ Pa s, $\Gamma = 2.3 \times 10^{-7}/t_0$. For these conditions, the region of basic frequencies whose spectral amplitudes exceed 10% of the maximum value is located between 2 and 100 Hz for $t_0 = 0.5$ s and between 20 Hz and 1 kHz for $t_0 = 0.05$ s.

The pressure gradient at the front, evaluated by formula (3), is $1.2 \times 10^6$ Pa/m for a peak pressure $p_0 = 200$ Pa and $3.2 \times 10^5$ Pa/m for $p_0 = 50$ Pa. The peak pressure falls during wave propagation, leading to a gradient decrease. For its evaluation, $p_0$ must be replaced by $p_0\sqrt{1+2z}$ in formula (3). For instance,

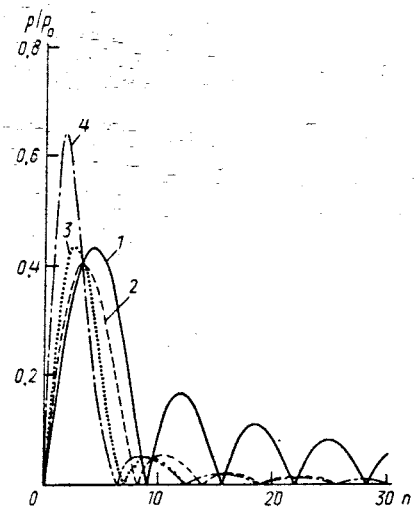


Fig. 1

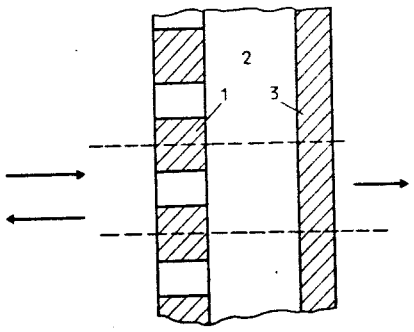


Fig. 2

at the distance $z = 0.5$ the gradient decreases by a factor of 2.8 with respect to its initial value; at $z = 1$ it decreases by a factor of 3.5.

However, it should be pointed out that if one takes into account the relaxation processes which take place in the atmosphere during wave propagation, the fronts may suffer additional widening. The pressure gradients would then be significantly lower than under ordinary atmospheric conditions.

Our analysis of the spectrum of a sound-shock wave (an $N$ pulse) shows that a significant fraction of the pulse energy is located in the low-frequency region. Therefore for shock wave absorption absorbers with low-frequency absorption characteristics should be employed, such as Helmholtz resonators. Also, some construction elements can be modeled with the aid of such a resonator or a system of such resonators. Thus, the effects of shock waves on a Helmholtz resonator must be studied both for solving the problem of shock wave absorption and for calculating pulses reflected by the structures. Such a system of sound absorbers is shown in Fig. 2. It consists of a perforated wall *1*, a cavity *2*, and a solid wall *3*. Since the incident pulse is assumed to have a flat front, the wave incidence problem can be solved for each cell individually (a cell is outlined by dashed lines). Partitions can be installed between the cells. One cell of this type will be a simplest model of a Helmholtz resonator (if such a model is applied to a room, the window cavity will be its throat).

Let an $N$ pulse of a given shape (Fig. 3, curve 1) with an infinitely narrow front be incident on the resonator. In order to be able to use the techniques of spectral analysis, let us assume that the resonator model has no nonlinearity. Then the system of equations for the variables $u$ (the wall velocity) and $V$ (the

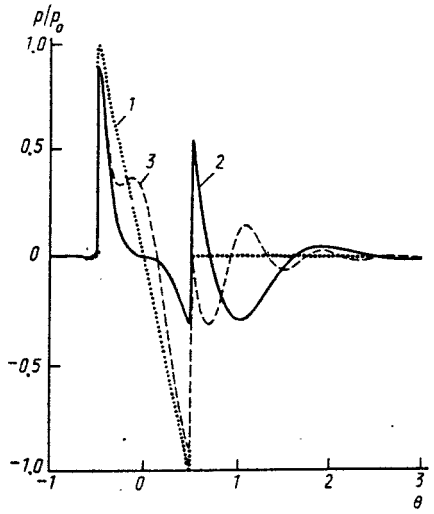


**Fig. 3**

medium velocity in the resonator throat, averaged over the volume) has the form [7]

$$\begin{aligned}
&\frac{d^2u}{dt^2} + 2\delta_1\frac{du}{dt} + \omega_{01}^2 u = \varkappa_1 V,\\
&\frac{d^2V}{dt^2} + 2\delta_2\frac{dV}{dt} + \omega_{02}^2 V + \frac{1}{a_1}\sqrt{\frac{\nu}{\pi}}\frac{d}{dt}\int\limits_{-\infty}^{t}\frac{dV}{dt'}\frac{dt'}{\sqrt{t-t'}}\\
&\qquad = \frac{2}{\rho_l L}\frac{dp_i(t)}{dt} + \varkappa_2 u,
\end{aligned} \tag{5}$$

where $\omega_{01}$ and $\omega_{02}$ are the wall and throat natural frequencies in the absence of nonlinearity and friction, $\delta_1$ and $\delta_2$ are the losses through friction and radiation (the wall friction can be accounted for by adding the friction coefficient to $\delta_1$), $\varkappa_1$ and $\varkappa_2$ are the coefficients of coupling between the two oscillatory circuits, $p_i$ is the incident wave pressure, $L$ is the resonator throat length. The integral term in the equation for oscillations in the throat describes the friction of the acoustic boundary layer [7].

Now the following expressions can be derived for the frequency dependencies of the absorption coefficient $K_r = p_r/p_i$ and the sound "transmission" coefficient $K_t = p_t/p_i$ ($p_r$ and $p_t$ are the pressures in the reflected and transmitted waves)

$$\begin{aligned}
K_r &= 1 - \frac{4i\Omega(\Omega_{01}^2 - \Omega^2 + 2i\Delta_1\Omega)}{(\Omega_{01}^2 - \Omega^2 + 2i\Delta_1\Omega)(\Omega_{02}^2 - \Omega^2 + 2i\Delta_2\Omega - \Omega^{3/2}V(1-i)) - K_1K_2},\\
K_t &= \frac{4i\Omega K_1}{(\Omega_{01}^2 - \Omega^2 + 2i\Delta_1\Omega)(\Omega_{02}^2 - \Omega^2 + 2i\Delta_2\Omega - \Omega^{3/2}V(1-i)) - K_1K_2},
\end{aligned} \tag{6}$$

where the following dimensionless variables have been introduced

$$\begin{aligned}
&\tau = \frac{2\rho_l L}{\rho_0 c_0}, \quad \Omega = \omega\tau, \quad \Omega_{01} = \omega_{01}\tau, \quad \Omega_{02} = \omega_{02}\tau, \Delta_1 = \delta_1\tau, \quad \Delta_2 = \delta_2\tau,\\
&V = \sqrt{\frac{\nu\tau}{2a_1^2}}, \quad K_1 = \varkappa_1\tau^2, \quad K_2 = \varkappa_2\tau^2.
\end{aligned} \tag{7}$$

Here $\omega$ is the incident wave frequency, $\rho_l$ and $\rho_0$ are the medium density in the resonator throat and the air density, $c_0$ is the velocity of sound in air.

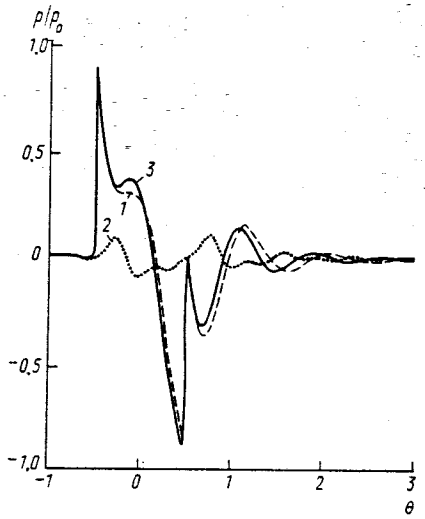


Fig. 4

Let the resonator back wall be immobile. Then $\Omega_{01} = 0$, $\Delta_1 = 0$, $K_1 = 0$. Knowing the incident pulse spectrum and the resonator frequency response, one can calculate the shape of the reflected pulse. The calculated shape is shown in Fig. 3 (curve 2). If the resonator's natural frequency (in the absence of absorption and nonlinearity) is twice as high, the shape of the reflected pulse will be different. This case is shown by curve 3 in Fig. 3.

If the resonator back wall is mobile, then, in addition to the reflected wave, the transmitted wave will also appear. The calculated results for such a system, for the same shape of the incident pulse, are shown in Fig. 4. Here curve 1 is the reflected pulse shape, curve 2 is the transmitted wave, and curve 3, shown for comparison, is the curve for a system with the same parameters but an immobile wall. Figure 4 shows that the reflected pulse changes when the wall mobility is taken into account. The wave that has passed the resonator has no steep fronts, because the Helmholtz resonator resonance frequency response transmits only a limited frequency range.

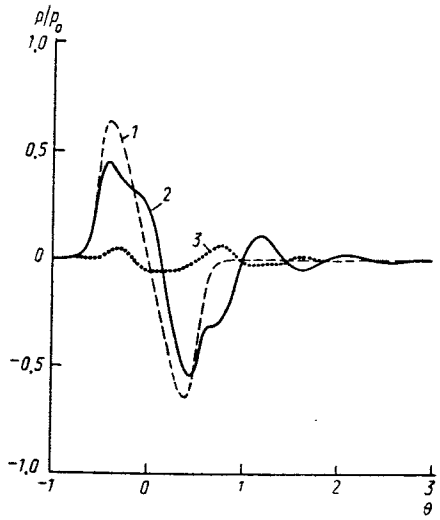


Fig. 5

Analyzing the shapes of reflected pulses, one can conclude that the pressure amplitude at the discontinuities decreases, which is evidence for energy absorption. Furthermore, the initial pulse acquires a "tail" which is due to the resonator's natural vibrations induced by the pulse. The energy of these vibrations is pumped from the main pulse, therefore one can speak of a decrease in the energy of the $N$ pulse and an increase in the duration of its action.

Unfortunately, in this case the steepness of the discontinuity fronts (i.e., the spatial gradient of discontinuity) does not decrease if a Helmholtz resonator is used as an absorber. This is due to the fact that the Helmholtz resonator has a low-frequency reflection characteristic, while the steepness of discontinuity depends on high frequencies (see above). A possible solution for this problem could be the use of combined absorbers, consisting of resonators and ordinary types of absorbers (e.g., porous or fiber structures) with higher-frequency reflection characteristics.

The situation changes if the incident $N$ pulse has a front of finite thickness (i.e., dissipation in the medium). This case is shown in Fig. 5. Here curve 1 is the incident pulse. Its spectrum is given by formula (4), in which it is assumed that $\Gamma = 0.03$, $z = 0$. The frequency dependencies of the resonator parameters are the same as in the previous case. Since the shock wave spectrum is bounded due to dissipation, the frequency interval in which absorption occurs covers it completely. Therefore absorption occurs over the entire front of the shock pulse, as seen from the shape of the reflected pulse (Fig. 5, curve 2). Taking dissipation into account does not lead to any qualitative changes in the shape of the transmitted wave (Fig. 5, curve 3). As in the previous case, the transmitted wave is not a shock wave, and with an appropriately chosen transmission coefficient its front will be much less steep than that of the incident pulse.

This research was supported by the Russian Foundation for Fundamental Research (Project no. 93-02-15453) and the Center for Fundamental Natural Sciences.

## REFERENCES

1. D. J. Maglieri, *J. Acoust. Soc. Am.*, vol. 92, no. 4(2), p. 2328, 1992.
2. A. D. Pierce, in: *Advances in Nonlinear Acoustics. World Scientific*, p. 7, 1993.
3. K. A. Velizhanina and D. A. Dudkin, *Akust. Zh.*, vol. 35, no. 1, p. 151, 1989.
4. D. A. Dudkin, Ph. D. Phys.-Math. Thesis, Moscow State University, Moscow, 1988.
5. K. Khirnykh, *The Development of Non-Fiber-Filled Resonant Sound Absorbing Systems: Ph. D.*, Institute of Environmental Engineering, South Bank Polytechnic, London, January 1992.
6. E. A. Lapshin, in: *Methods and Algorithms in Numerical Analysis* (in Russian), p. 183, Moscow, 1984.
7. O. V. Rudenko and K. L. Khirnykh, *Akust. Zh.*, vol. 36, no. 3, p. 300, 1990.

29 March 1995

Department of Acoustics